

Spatial and Temporal Distribution Characteristics of Electric Vehicle–Grid Interaction Scheduling Using Cluster Optimization

Tao Huang*

Chongqing Three Gorges Vocational College, Chongqing 404155, China

(Received January 7, 2023; accepted April 26, 2023)

Keywords: electric vehicles, cluster optimization, power allocation, microgrid, scheduling strategy

The disorderly access of large-scale electric vehicles (EVs) will have adverse effects on the microgrid, such as increasing the peak-valley difference, decreasing the power quality, and increasing the difficulty in microgrid operation optimization and control. To this end, the author proposed an EV to microgrid (V2M) interaction scheduling strategy using cluster optimization to balance power demand and supply in the microgrid. First, in the lower-level vehicle-to-aggregator (V2A) stage, the EVs in each period are dynamically divided into regular and regulated clusters according to their battery, time, and charging/discharging conversion time constraints, with the regular cluster carrying out disorderly charging and the regulated cluster containing charging and discharging clusters. Then, in the upper-level aggregator-to-microgrid (A2M) stage, the dispatchable load of the control cluster is optimized at the control center to minimize the total load variance during the study period, using the cluster division and cluster load information as constraints. Finally, the power allocation algorithm is used to realize the spatial and temporal distributions of the EV cluster charging demand and discharging capacity for the scheduling strategy of V2A and A2M interactions. The proposed method can ensure that the EVs can cut the peak and fill the valley of the microgrid while meeting the travel demand.

1. Introduction

The power demand from the electric vehicle (EV) charging load has the potential to cause a large burden on the power system. As EVs are further promoted on a large scale, the impact on the electric power system is likely to increase. At the same time, EVs are also highly flexible mobile energy storage units, which have considerable potential to adjust electricity loads, improve power quality, and absorb renewable energy, and can also help reduce the expansion needs of distribution networks and even the entire network.

The vehicle-to-microgrid (V2M) technology is a new type of microgrid technology⁽¹⁾ that can embody the flow of energy between vehicles and the microgrid in a bidirectional, real-time, controlled, and high-speed manner, and is an effective way to solve the above problems. The V2M technology is applied to control the charging and discharging of EVs, and the microgrid dispatches EV charging to store excess power generation from the microgrid during low-load

*Corresponding author: e-mail: 13884897@qq.com
<https://doi.org/10.18494/SAM4315>

periods and feeds electricity from EVs to the microgrid during the peak load period, which can, on the one hand, mitigate the negative impact of EV scale development on the power system.⁽²⁾ On the other hand, it can also reduce the total charging cost and system network loss, and play a role in peak shaving and valley filling. Moreover, it can reduce the total charging cost and system network loss, and play the role of peak shaving and valley filling to smooth out the intermittent and volatile nature of renewable energy.⁽³⁾ Under the V2M model, the orderly dispatch of large-scale EVs can bring economic benefits to the microgrid and users, achieve mutual benefits, and promote the development of EVs.

When a large number of EVs are connected to the microgrid for charging at the same time, a load peak will form, which is unacceptable to the distribution microgrid, causing interference to the normal operation of the distribution microgrid and further causing power quality problems such as line overload, voltage instability, harmonic pollution, and network loss.^(4,5) To facilitate the management of large-scale EVs with decentralized and random characteristics, the concept of the EV aggregator is proposed,⁽⁶⁾ i.e., a cluster formed by aggregating a certain number of EVs that can provide a certain scale of dispatchable capacity to interact with the microgrid and participate in the power market. Therefore, it is more meaningful to predict the charging load of EVs, analyze the impact of disorderly charging on the microgrid, formulate strategies for the interaction between EVs and the microgrid, and help the microgrid achieve a stable operation through peak regulation and frequency regulation.

In the system of V2M interaction, EV agents manage regional EV clusters and participate in electricity market transactions, interact with the microgrid (aggregator-to-microgrid, A2M)⁽⁷⁾ at the upper layer, and interact with an EV (vehicle-to-aggregator, V2A)⁽⁸⁾ at the lower layer, playing a key role in bridging EV clusters and the microgrid and forming a hierarchical network–business–vehicle interaction architecture, as shown in Fig. 1. In the upper layer of the vehicle–net interaction, the EV agent provides the dispatchable power of the vehicle fleet at different time scales to the microgrid, and EV agents compete with each participating entity in the electricity energy market and ancillary services market for revenue. In the lower layer of the V2M interaction, EV agents formulate individual EV charging and discharging guidance mechanisms according to the dispatching strategy to motivate users to participate in the positive microgrid interaction and realize the optimal dispatching of EV charging and discharging. For the scheduling strategy of V2A and A2M interactions, the existing research on V2M load prediction and its interaction with the microgrid focuses on the following three aspects: research on the spatial and temporal distributions of EV cluster charging demand and discharging capacity,⁽⁹⁾ V2M-based cooperative scheduling strategy,⁽¹⁰⁾ and market mechanism and economic cooperation.⁽¹¹⁾

For EV charging and discharging control, two aspects have been studied, group scheduling and individual scheduling. Individual scheduling is suitable for control scenarios with small vehicle sizes. Ansari *et al.* established a real-time scheduling model for charging and discharging optimization for the travel demand conditions of each EV, which can satisfy the charging demand of each EV, but when the number of vehicles on the microgrid increases, the increase in variable dimensions will increase the computational volume exponentially and make the solution difficult or even impossible.⁽¹¹⁾ Group scheduling, on the other hand, clusters the EVs in the

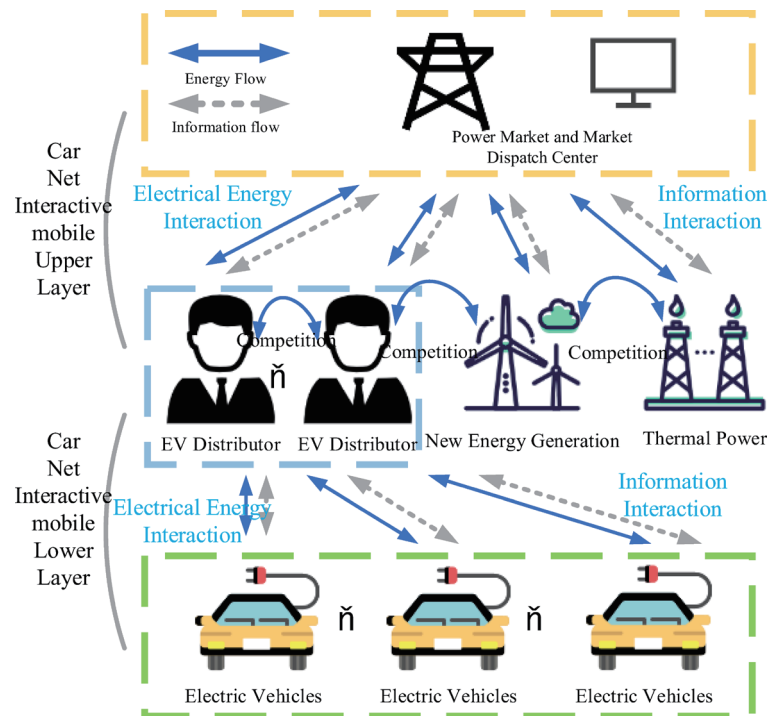


Fig. 1. (Color online) Schematic diagram of hierarchical scheduling of EV-grid interaction.

microgrid and schedules the group as a whole. The cluster scheduling is based on travel characteristics such as the end moment of EV travel and the required charging duration, and a delayed charging and discharging strategy is developed for each EV within each subcluster.⁽¹²⁾ The scheduling plan of each EV agent is optimized in the upper-level model, whereas the charging and discharging time is optimized for the EV under the agents in the lower-level model.⁽¹³⁾ According to the expected charging completion time of the connected EVs, which are divided into several EV clusters with different priorities, an EV population optimization model is established to minimize load variance.⁽¹⁴⁾ Although the above group scheduling strategy can reduce the complexity of model solution calculation, it does not consider the scheduling priority of a single EV within the cluster and the fairness of energy distribution.

Overall, the main contributions of this study are as follows: (I) To address the above problems, in this work, the author conducted research on the specific power allocation of a single EV during charging and discharging, combined the principle of cluster scheduling, dynamically adjusted the charging and discharging state of EVs according to the real-time load, and proposed a subcluster optimized V2M method. (II) The author divided EVs into clusters according to a large amount of aggregated charging information, e.g., the remaining battery capacity and time constraints, the actual situation of the current microgrid and the power demand, and charging and discharging capacity of each subgroup, then optimally controlled the total charging and discharging power of EVs, and next generated a power allocation algorithm to fairly control the charging and discharging of each EV. (III) Compared with both the valley searching optimization

algorithm and the charge and discharge rate adjustable optimization algorithm, the simulation results showed that the proposed strategy can effectively reduce load change, realize peak shaving and valley filling, and reduce charging costs while ensuring customer satisfaction.

2. System Architecture under the “Vehicle-Road-Net” Model

The EV charging load in the “vehicle-road-net” model has dual attributes in the same time scale: one is the spatial distribution characteristics, including real-time location, destination, and driving speed; the other is the energy attributes, including energy consumption per unit mile, real-time power, and range. The topology of the traffic network and the degree of road saturation directly affect the spatial attributes of EVs, whereas the driving path length determined by the spatial attributes affects the energy attributes of EVs, and battery power, in turn, affects the spatial distribution of EVs. Therefore, the energy attributes of EVs correspond to “when” and the spatial attributes correspond to “where”; the two jointly determine the spatial and temporal distribution characteristics of the EV charging load. Given the differences in the spatial and energy attributes of different types of EV, the charging load of large-scale EVs will have clear spatial and temporal distribution characteristics.

To simplify the analysis, the author assumed that EV charging facilities can be well distributed and configured in an urban road network,⁽¹⁵⁾ i.e., the study of the spatial and temporal distribution characteristics of the charging load is not limited by the location and capacity of charging stations. Moreover, the urban road network and distribution network nodes are geographically coupled,⁽¹⁶⁾ and EVs can be charged at a nearby charging facility when the battery is low, and the charging facility is connected to the nearest distribution network node.

2.1 Single EV charging model

2.1.1 EV classification

According to the TranCAD software description and the classification statistics of the UK Department for Transport, considering the current situation of the use and development of EVs in China, the author divided EVs into three categories according to their travel characteristics: private cars (travel between workplace and residence on weekdays, and go out for leisure on rest days, including A and B cars), official cars (travel between workplaces on working days, no travel on rest days, including both A and B cars), and taxis (multiple trips in a day, with random destinations, running daily, including only B cars). Class A vehicles refer to EVs with fixed slow-charging equipment, which are charged slowly at night in their parking spaces to meet the electric energy demand. Class B vehicles refer to EVs without fixed slow-charging equipment, which are charged quickly at charging stations when the remaining power is low, and their energy replenishment method is similar to the gasoline vehicle refueling method.

2.1.2 Main state parameters

Through an in-depth investigation of EVs, the database provided by the EU Seventh Framework MERGE project encompasses the parameters of EVs produced by all major manufacturers in the current market. In this study, the author defined the state parameters of EVs, including location and power status information, which can be represented by the set of state parameters of EVs $\{O_i, t_s, L_t, Cap_r, Cap_0, Cap_t, \Delta Cap, R\}$. In this study, the author used the probability distribution curves of the initial travel time t_s and return time t_f for each type of EV on a typical weekday provided by the National Cooperative Highway Research Program (NCHRP187) in TranCAD to generate the initial travel time of EVs. According to the data analysis of the EV database of the MERGE project, the battery capacity $Cap_r^{\alpha-1}$ of different types of EV obeys the gamma distribution of “[Eq. (1)]” or the normal distribution of “[Eq. (2)]”.

$$f(Cap; \alpha, \beta) = \frac{1}{\beta^\alpha \Gamma(\alpha)} Cap_r^{\alpha-1} e^{-\frac{Cap_r}{\beta}} \quad (1)$$

$$g(Cap; \mu, \sigma) = \frac{1}{\sigma\sqrt{2\pi}} e^{-\frac{(Cap_r - \mu)^2}{2\sigma^2}} \quad (2)$$

Suppose that the initial state of charge (SOC) of an EV is the charge level that has just been charged. To prevent damage to the battery caused by overcharging, the SOC of the EV after charging is set in the range of 0.8–0.9. According to the battery capacity of the EV, the initial charge Cap_0 can be obtained by combining the initial SOC.

In this study, assuming that the power consumption of an EV increases linearly with the distance traveled, the remaining power at time t can be calculated using Eq. (3), where Cap_{t-1} represents the remaining power at the last sampling moment $t - 1$, Δl represents the distance traveled from time $t - 1$ to time t , and the energy efficiency coefficient η is introduced to characterize the power loss caused by starting and braking during the actual driving process. The energy efficiency coefficients are taken in the range of 0.9–1.

$$Cap_t = \eta(Cap_{t-1} - \Delta l \cdot \Delta Cap) \quad (3)$$

2.2 Regional traffic road model

2.2.1 Road topology diagram

Suppose that the area is a two-way road, and an undirected graph is used to represent its topology. The road diagram is represented as $G = (U, E)$, where U represents the set of nodes in the undirected graph, that is, the start and end points or intersections of roads, numbered 1, 2, ...,

H , and E is the edge set, i.e., the relationship between vertices. When the weighted graph is represented by the adjacency matrix, $G = (U, E)$ corresponds to a matrix E of order $H \times H$. The weight function of the road network is denoted by ω , i.e., the road resistance function. The assignment rule of the E element d_{ij} in the adjacency matrix is defined as follows.

$$d_{ij} = d_{ji} = \begin{cases} \omega_{ij} & i \neq j, (i, j) \in E \\ 0 & i = j \\ \omega_{inf} & i \neq j, (i, j) \notin E \end{cases} \quad (4)$$

Here, ω_{ij} is the weight between road nodes i and j , and ω_{inf} denotes the road section without a direct connection between the two nodes.

2.2.2 Road resistance function model

In traffic networks, travel time is mainly limited by the road class, intersection traffic lights, and traffic flow. The Logit-based traffic delay function is used to represent the road resistance model of the road, with nodes i and j as the endpoints of the directly connected road sections, and the time spent by vehicles traveling from node i to node j is represented by the total delay function of the road section as

$$T(i, j) = 60 \cdot [L(i, j) + I(i, j)], \quad (5)$$

where $T(i, j)$ presents the total delay time of the road segment and intersection, $I(i, j)$ the intersection delay time, and $L(i, j)$ the road segment delay time, as shown in Eq. (6).

$$\begin{cases} L(i, j) = L_0 \cdot c_1 \frac{[1 + \exp(c_3 - c_4 \lambda_L)]}{-c_2 + [1 + \exp(c_3 - c_4 \lambda_L)]} \\ \lambda_L = \frac{q_{ij}}{C_{ij}} \end{cases} \quad (6)$$

Here, L_0 is the road section free-flow travel time, q_{ij} is the road flow, i.e., the number of cars passing through the road section per hour, which can be obtained by manual observation or by using a traffic flow meter, and C_{ij} indicates the road section traffic capacity. c_1 , c_2 , c_3 , and c_4 are the adaptive coefficients under different road classes, which are related to the road class. In addition, $I(i, j)$ denotes the intersection delay time, mainly considering the traffic light factor, as shown in Eq. (7).

$$\begin{cases} I(i, j) = I_0 \cdot p_1 \left\{ 1 + \frac{p_2}{1 - \exp(p_3 - p_4 \lambda_I)} \right\} \\ \lambda_I = \frac{q_{ij}}{X_{ij}} \end{cases} \quad (7)$$

Here, I_0 defines the intersection free-flow travel time, X_{ij} presents the roadway capacity, and p_1 , p_2 , p_3 , and p_4 are the adaptive factors of the intersection, which are related to the presence or absence of traffic lights.

2.2.3 Path selection

The weight of the path $p = (v_1, v_2, \dots, v_k)$ refers to the sum of the weights of the edges passing from the origin v_1 to the destination v_k , i.e.,

$$\omega(p) = \sum_{i=2}^k \omega(v_{i-1}, v_i). \quad (8)$$

The weight $\sigma(i, j)$ of the shortest path from node i to node j is defined as

$$\sigma(i, j) = \begin{cases} \min \{ \omega(p) : i \rightarrow j \} & (i, j) \in E \\ \omega_{int} & (i, j) \notin E \end{cases}. \quad (9)$$

The weights of the edges are expressed using the traffic delay function described by the road resistance function model, i.e., $\omega(p) = T(i, j)$. The goal is the shortest travel time to be achieved using the Dijkstra algorithm to select the optimal path. Suppose that the set of the shortest time-consuming paths between nodes i and j contains n directly connected segments, and the travel time ΔT_s of the s th section is found by the Logit-based traffic delay function. The distance Δl_s of the s th directly connected section is a known quantity. Then, the total travel time ΔT_{ij} and the total travel distance Δl_{ij} between nodes i and j are defined as

$$\begin{cases} \Delta T_{ij} = \sum_{s=1}^n \Delta T_s \\ \Delta l_{ij} = \sum_{s=1}^n \Delta l_s \end{cases}. \quad (10)$$

In practice, users do not always choose the path with the shortest travel time for personal reasons, and considering the diversity of the paths chosen by users, the shortest time-consuming path is defined as the path chosen by users with high probability, while the probability of

choosing other paths is the same and uniformly distributed. If the user has m ($m > 1$) types of path set from the starting point to the destination, then the probability that the user chooses the path with the shortest travel time is P_m and the probability that the user chooses other paths is $(1-P_m)/(m-1)$, and in this study, the author takes $P_m = 0.8$.

2.3 Microgrid modeling based on graph theory approach

In this study, the microgrid is modeled by simplifying it to a network structure consisting of nodes and arc segments, without considering switches, and the nodes represent only generators and loads. The topology of the microgrid is shown in Eq. (11).

$$\left\{ \begin{array}{l} G^d = \left((V^d(G)), (E^d(G)), (\Psi_G^d) \right) \\ V^d(G) = \{n_i | i = 1, 2, \dots, n_G\} \\ E^d(G) = \{ \langle n_i, n_j \rangle | n_i, n_j \in V^d \} \\ \Psi_G^d = \{ (r_i, x_i, c_i, P_i^d) | \langle n_i, n_j \rangle \in E^d \} \\ B_G^d = \{ (P_i^d, Q_i^d) | i = 1, 2, \dots, n_G \} \\ F_G^d = \{ f_i(t) | t = 1, 2, \dots, T \} \end{array} \right. \quad (11)$$

Here, $V^d(G)$ is the set of nodes of the microgrid, n_G is the number of microgrid nodes, $E^d(G)$ is the set of branches between microgrid nodes, Ψ_G^d is the matrix of parameters such as the resistance, reactance, electron agogic, and branch transmission power limit of the microgrid branches, B_G^d is the average active and reactive power of each node in the microgrid, F_G^d describes the coefficient of load variation of the microgrid nodes, T defines the total time of day, and l_d presents the number of branches.

3. Clustering-enabled V2M Participation in Microgrid Peak-shaving and Valley-filling Research

3.1 Cluster optimization ideas

The purpose of this study is to make full use of the adjustable EV charging time and maximize the energy storage potential of EVs to achieve peak and valley reduction. The idea of the optimal scheduling of EVs in clusters is shown in Fig. 2.

The specific implementation steps of the cluster optimization idea are as follows.

- (1) Data acquisition: The real-time load information of the microgrid is obtained through the electricity information acquisition system; the battery information of the connected vehicle, including rated power, battery capacity, battery charge status, etc., is obtained through the

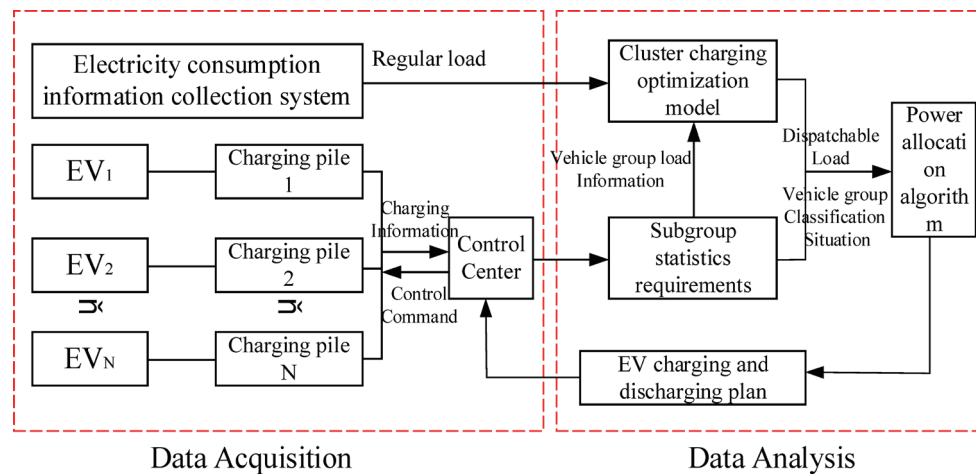


Fig. 2. (Color online) Group-based optimization scheduling idea of EVs.

battery management system of EVs. Meanwhile, the user inputs the travel data, e.g., the expected state of electric quantity and the expected time of picking up the EVs, through the human–computer interaction interface on the charging pile, as well as the information, e.g., whether to accept the regulation service for the grid.

- (2) Data analysis: The microgrid and charging information is uploaded to the control center through wired or wireless communication, and the historical travel and charging completion data are extracted to establish a historical dynamic scheduling strategy model of EVs at the control center. The strategy model includes the subgroup charging optimization model and power allocation algorithm.
- (3) Program execution: The charging and discharging plan updated by the control center according to the time slot is released to the charging pile, and the charging and discharging functions and input and output powers of the charging pile are controlled to control the charging and discharging behaviors of EVs

In this study, on the basis of microgrid and real-time input information of vehicles, the demand statistics and charging optimization model of subgroups are dynamically updated by the control center, and the charging and discharging tasks of EVs are centrally regulated according to the fluctuation condition of the microgrid. The 1-d time slot is divided into multiple charging control periods, and the charging and discharging schedules of EVs in each control period are optimized separately. The time slot length Δ (t in min) for updating the data information should be determined on the basis of the actual vehicle access situation. In this work, the study control time is 00:00–24:00 and the number of study control periods is $24 \times 60/\Delta t$. The serial number of the periods is denoted by n ; for example, $n = 1$ means period 1, i.e., 00:00–01:00.

3.2 Cluster discriminatory criteria

According to the properties of EVs, the control center integrates four indicators, namely, vehicle type, charge status, parking duration, and vehicle owner's intention, and classifies EVs in

time slot n into the conventional (nonregulated) vehicle group S_1 and regulated vehicle group S_2 . S_1 has the absolute nature of being nonregulated, and when the charging pile detects that the connected EV meets the criterion S_1 , it will automatically enter the charging mode until it meets the charge status requirement or reaches the travel time. The charging pile provides bidirectional power flow to the operating microgrid for peak regulation or provides ancillary services for the microgrid, and the charging start time of this fleet can be flexibly adjusted before the travel moment. Therefore, when the charging pile detects that the connected EV meets the criterion S_2 , it will be in the phase of waiting for the charging and discharging commands to be issued as shown in Fig. 3.

3.3 Charging optimization model

The control center optimally limits the load of each vehicle group according to the load information of each vehicle group and the conventional load information. However, the conventional vehicle group S_1 is only connected to the microgrid as a charging load and does not participate in microgrid dispatching, so the charging power of the conventional vehicle group is not restricted. S_2 is the main force participating in the peak and valley reduction of the microgrid, so it is necessary to calculate which schedulable load limit is used to control the orderly charging and discharging of the regulating vehicle group to minimize the load fluctuation.

Assuming that the time-sharing discharge tariff is equal to the charging tariff, the optimization model for the time slot n is established so that the overall load variance of the microgrid for time slots $1 - n$ is the lowest and the total cost of charging involved in regulation is lower than that of disorderly charging, and the optimization variable is the dispatchable load

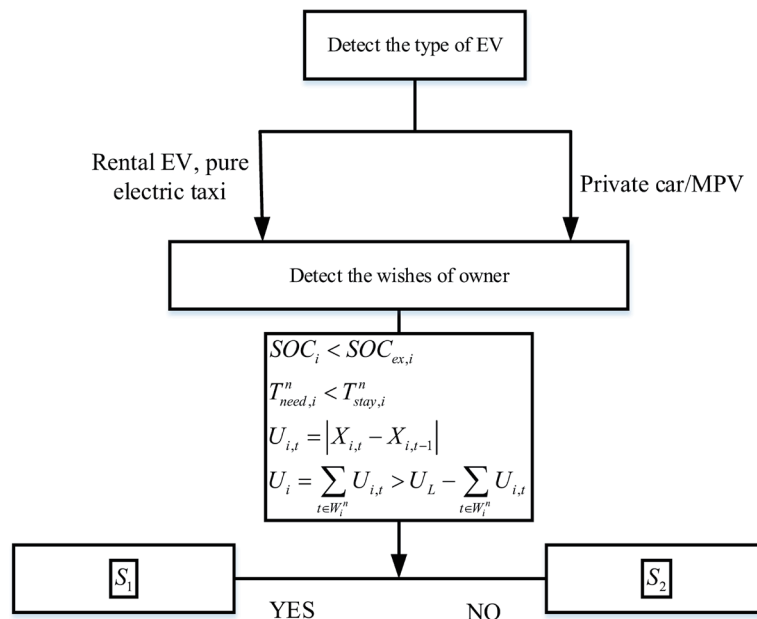


Fig. 3. Cluster discriminant standard order.

limit P_{V2G}^n of the regulation vehicle group S_2 for the time slot n . The optimization model for the time slot n is defined as follows.

$$\begin{aligned}
 P_{V2G}^n (op) &= \arg \min J(P_{V2G}^n) \\
 s.t. \quad P_{S_{22}}^n &\leq P_{V2G}^n \leq P_{S_{21}}^n \\
 \sum_{j=1}^n (P_{S_1}^j + P_{V2G}^j) \Delta t^j c^j &< \sum_{j=1}^n P_{wx}^j \Delta t^j c^j \\
 J(P_{V2G}^n) &= \sum_{j=1}^n (P_{LD}^j + P_{S_1}^j + P_{V2G}^j - P_{av}^n)^2 \\
 P_{av}^n &= \frac{1}{n} \sum_{j=1}^n (P_{LD}^j + P_{S_1}^j + P_{V2G}^j)
 \end{aligned} \tag{12}$$

Here, P_{LD}^j and P_{wx}^j are the total load required for a regular load and EV disorderly charging in kW for the time slot j , respectively, P_{V2G}^j is the dispatchable load limit in kW for the vehicle group S_2 in the time slot j , Δt^j is the time duration of the time slot j , and c^j is the time division tariff of the time slot j .

3.4 EV charging and discharging schedule

The conventional vehicle group S_1 is autonomously sensed by the charging pile and adopts the disorderly charging mode. After solving the optimization model to obtain the optimal dispatchable load of the period n , the control center determines the charge and discharge state of the regulated vehicle group S_2 and the fair regulation of the charge and discharge power of each EV in the group according to this value, and sends the charge and discharge plan to the charging pile connected to the regulated vehicle group. The band-weighted maximum and minimum fair allocation algorithm schedules limited resources according to user weights and is a scheduling algorithm used to solve the problem of fair bandwidth allocation between resources in wireless communication. Therefore, in this study, we combined the weighted max–min fair distribution algorithm to achieve a fair distribution of limited power resources, and the charge–discharge scheme S_2 is formulated in Fig. 4.

4. Results and Discussion

4.1 Parameter setting

For example, the distributed generation source of the microgrid in a region consists of 60 wind turbines and 1000 photovoltaic arrays; the rated power of a single wind turbine is 100 kW, and its corresponding cut-in wind speed, cut-out wind speed, and rated wind speed are 3.5, 25 and 15 m/s, respectively. The photovoltaic arrays are composed of 4×5 photovoltaic battery

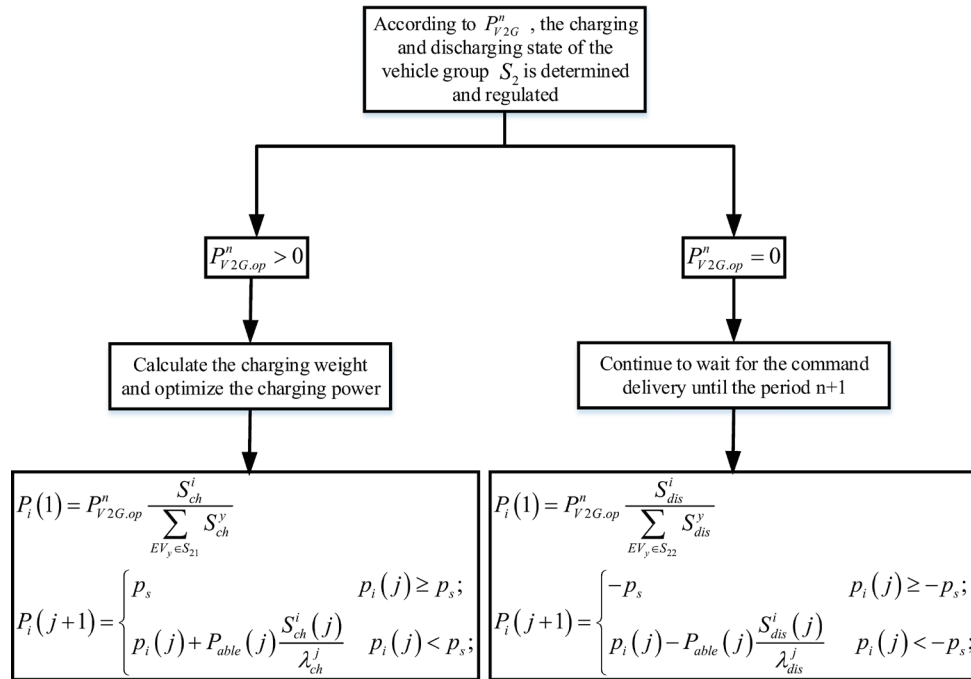


Fig. 4. EV charge–discharge plan flowchart.

panels, and their rated power is 4 kW. The number of EVs in the region is 2000, the capacity of the battery is 20 kWh, the price is 2000 RMB/(kWh), and the maximum number of charges/ discharges is 1000. According to relevant information, the average daily driving distance of a private car is about 40 km, namely, the distance to and from work is 20 km, the battery of an electric car consumes 0.15 kWh per kilometer, and the electric car needs to consume 3 kWh for commuting, which is converted to the charge state of 0.15. Therefore, to ensure safe travel, the initial charge state of the battery is set to 0.6 and the minimum charge state of the battery is set to 0.2. The rated charge/discharge rate of the EV battery is 0.2 C (4 kW) and the maximum charge/discharge rate is 0.25 C (5 kW).

4.2 EV charging and discharging schedule

To visualize the control effect of the cluster optimization scheduling scheme, the time slot length of the updated data is assumed to be 15 min. According to the cluster optimization flow shown in Fig. 5, the timing simulation of the cluster optimization scheduling of EVs is performed for each time slot and compared with the default unordered charging mode adopted before cluster optimization. In the unordered charging mode, the charging time of EVs is not limited, and users are used to charging EVs at rated power immediately after they are connected to the charging pile until the charge state reaches the maximum allowed value or is close to the travel departure time. To verify the practicability of the proposed algorithm, the clustering optimization algorithm, the valley-seeking optimization algorithm, and the charge–discharge rate adjustable optimization algorithm are used to compare the control effects. Figure 5 shows the daily load

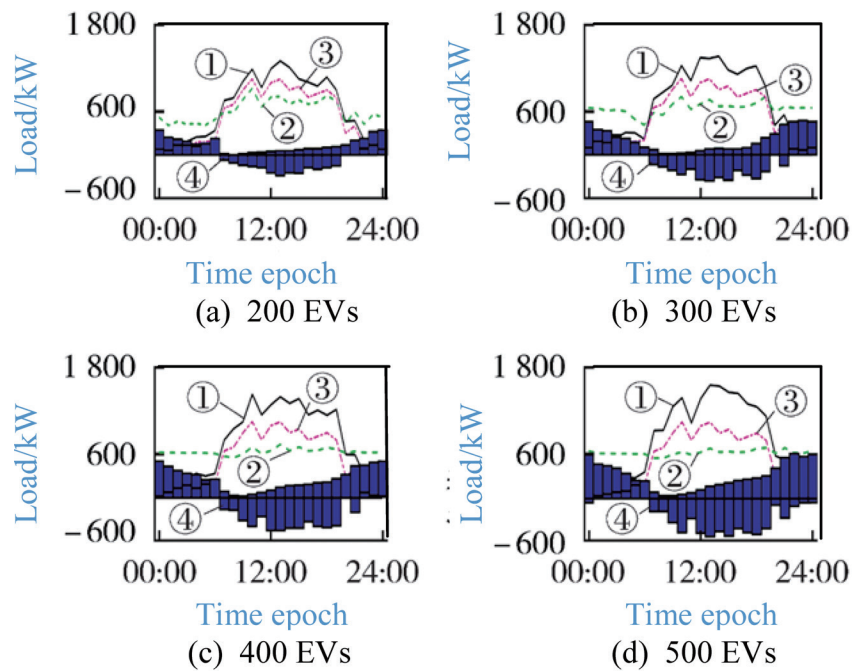


Fig. 5. (Color online) Load curves with different numbers of EVs. (1) Cluster optimization algorithm. (2) Valley searching optimization algorithm. (3) Charge and discharge rate adjustable optimization algorithm. (4) EV charging and discharging load.

distributions of EVs when the charging scales are 200, 300, 400, and 500. It can be seen from Fig. 5 that (1) before adopting the cluster optimization scheme, the charging load peaks of EVs in the commercial area in the disorderly charging mode will overlap with the original power consumption peaks of the microgrid, and this leads to an increase in the peak-valley difference of the load in the commercial area, which will pose a threat to the power security of the microgrid. (2) After adopting cluster optimization management, the regulating vehicle group makes charging and discharging adjustments according to the fluctuation of the microgrid, and it relieves the power supply pressure of the microgrid, reduces the peak load during the peak period of electricity consumption, and stores the excess electricity generated by the microgrid during the trough period, which can considerably reduce the peak-valley difference of the microgrid and play the role of peak cutting and valley filling. (3) When the number of connected EVs increases, it can be seen from the changing trend of the curve that the use of the cluster optimal dispatching solution makes the load fluctuation close to smoothness, and the effect of peak and valley reduction is significant.

To maximize their benefits, it can be recommended that car owners can charge their EVs when electricity prices are low and sell electricity to the microgrid when electricity prices are high. The average monthly revenue obtained by each vehicle owner according to the data of the State Grid Chongqing Electric Power Company is shown in Table 1. When EVs in the microgrid do not participate in the charging and discharging schedule, the owner can only purchase electricity from the microgrid to meet the charging demand of their EVs, and the revenue is

Table 1
Average benefit of each EV owner per month.

Algorithm	Benefit
Cluster optimization algorithm (proposed)	78
Valley searching optimization algorithm	29
Charge and discharge rate adjustable optimization algorithm	-40

negative. When the vehicle owner participates in the V2M service, a certain revenue is obtained, but the additional charging and discharging of the battery occurs, which will increase the cost of battery loss. In the benchmark optimization algorithms, the charging and discharging schedule can be adjusted according to the actual situation.

5. Conclusions

In this paper, we proposed a V2M scheduling strategy combining cluster management and dynamic optimization to manage the connected EVs in clusters and adopt different charging schemes. In the cluster statistical model, EVs arriving at charging stations can be divided into regular and normative clusters, and the total demand load of the regular cluster and the total controllable load of the regulated cluster are determined. In the charging optimization model, the total controllable load of the regulated vehicle group is optimized, and the charging and discharging power of each EV is adjusted on the basis of the power allocation algorithm according to the calculated vehicle weights to ensure that the EV reaches the charge state desired by the user before leaving. The method proposed in this paper is simple and effective and provides reasonable guidance for the scheduling of each EV in the actual system. The strategy is also applicable to places where EVs are charged in a centrally controlled manner, such as company and residential parking lots. In the actual scheduling process, the actual charging parameters of EVs updated by time slots will update their charging and discharging schedules in real time to ensure users' travel demand. On the basis of battery constraint, time constraint, and the number of charge/discharge transitions of EVs, this strategy dispatches as many EVs as possible to peak-shave the microgrid while satisfying their charging demand.

Acknowledgments

This work was supported by the Science and Technology Research Program of Chongqing Education Commission (No. KJQN202003502) and the Scientific Research Program of Chongqing Three Gorges Vocational College (No. CQSX202009).

References

- 1 H. Turker and S. Bacha: IEEE Trans. Veh. Technol. **67** (2018) 10281. <https://doi.org/10.1109/TVT.2018.2867428>
- 2 K. Lai and L. Zhang: IEEE Trans. Ind. Appl. **57** (2021) 1909. <https://doi.org/10.1109/TIA.2021.3057339>
- 3 H. Ko, S. Pack, and V. C. M. Leung: IEEE Trans. Intell. Transp. Syst. **19** (2018) 2165. <https://doi.org/10.1109/TITS.2018.2816935>
- 4 N. Guo, X. Zhang, Y. Zou, B. Lenzo, G. Du, and T. Zhang: IEEE Trans. Transp. Electrification. **7** (2021) 2488. <https://doi.org/10.1109/TTE.2021.3085849>

- 5 I. Husain, B. Ozpineci, M. S. Islam, E. Gurpinar, G. Su, W. Yu, S. Chowdhury, L. Xue, D. Rahman, and R. Sahu: Proc. IEEE **109** (2021) 1039. <https://doi.org/10.1109/JPROC.2020.3046112>
- 6 S. I. Vagropoulos, D. K. Kyriazidis, and A. G. Bakirtzis: IEEE Trans. Smart Grid **7** (2016) 948. <https://doi.org/10.1109/TSG.2015.2421299>
- 7 K. S. Ko, S. Han, and D. K. Sung: IEEE Trans. Smart Grid **9** (2018) 866. <https://doi.org/10.1109/TSG.2016.2570242>
- 8 C. Wu, H. Mohsenian-Rad, and J. Huang: IEEE Trans. Smart Grid **3** (2012) 434. <https://doi.org/10.1109/TSG.2011.2166414>
- 9 K. P. Inala, B. Sah, P. Kumar, and S. K. Bose: IEEE Syst. J. **15** (2021) 3749. <https://doi.org/10.1109/JSYST.2020.3007320>
- 10 H. Krueger and A. Cruden: IEEE Trans. Veh. Technol. **69** (2020) 4727. <https://doi.org/10.1109/TVT.2020.2976035>
- 11 M. Ansari, A. T. Al-Awami, E. Sortomme, and M. A. Abido: IEEE Trans. Smart Grid **6** (2015) 261. <https://doi.org/10.1109/TSG.2014.2341625>
- 12 S. Han, S. Han, and K. Sezaki: IEEE Trans. Smart Grid **1** (2010) 65. <https://doi.org/10.1109/TSG.2010.2045163>
- 13 M. Wang, Y. Mu, Q. Shi, H. Jia, and F. Li: IEEE Trans. Smart Grid **11** (2020) 4176. <https://doi.org/10.1109/TSG.2020.2981843>
- 14 H. Wu, M. Shahidehpour, A. Alabdulwahab, and A. Abusorrah: IEEE Trans. Sustainable Energy **7** (2016) 374. <https://doi.org/10.1109/TSTE.2015.2498200>
- 15 Y. Mu, J. Wu, N. Jenkins, H. Jia, and C. Wang: Appl. Energy **94** (2012) 395. <https://doi.org/10.1016/j.apenergy.2013.10.006>
- 16 Y. Xiang, J. Liu, R. Li, F. Li, C. Gu, and S. Tang: Appl. Energy **178** (2016) 647. <https://doi.org/10.1016/j.apenergy.2016.06.021>

About the Author



Tao Huang received his B.S. degree in electronic information engineering from Chongqing Technology and Business University, China, and his M.S. degree in electronic and communication engineering from Chongqing University of Posts and Telecommunications, China, in 2005 and 2013, respectively. He was a visiting scholar focusing on applications of electronics at Chongqing University and on communication engineering and electrical, media, and information technologies at Technische Hochschule Deggendorf (Deggendorf Technical University) in 2015 and 2018, respectively. He is currently an associate professor at the Chongqing Three Gorges Vocational College. His research interests include electronics, communication, and automation. (13884897@qq.com)